Impact of Mountain Waves on the Spatio-Temporal Development of the Boundary-Layer over Corsica

Norbert Kalthoff[1] (norbert.kalthoff@kit.edu), Bianca Adler[1,2,3], Inge Bischoff-Gauß[4],

[1] Institute of Meteorology and Climate Research, KIT, Germany [2]CIRES, University of Colorado, Boulder, CO, USA [3]NOAA PSL, Boulder, CO, USA [4] Steinbuch Centre for Computing, KIT, Germany

Karlsruhe Institute of Technology

Motivation

Spatio-temporal differences of ABL conditions were observed in a valley on the island of Corsica (Fig. 1) on a cloud-free day with strong westerly flow.
The ABL development could not be fully explained by the measurements (Adler and Kalthoff, 2016).

Approach

(i) Perform high resolution simulations, **(ii)** validate the model simulations, **(iii)** combine model output and observations to understand the ABL development at the measurement sites, and **(iv)** investigate the spatio-temporal ABL evolution in the valley.

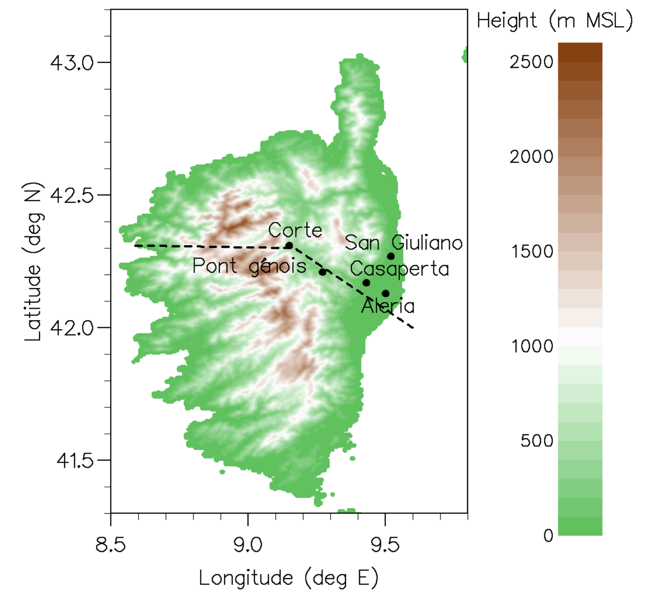

Fig. 1: Orography of Corsica, measurement sites (black dotes) and aircraft flight track (dashed line). Radiosonde (Corte, San Giuliano) and surface stations (Corte, Pont génois, Casaperta and Aléria).

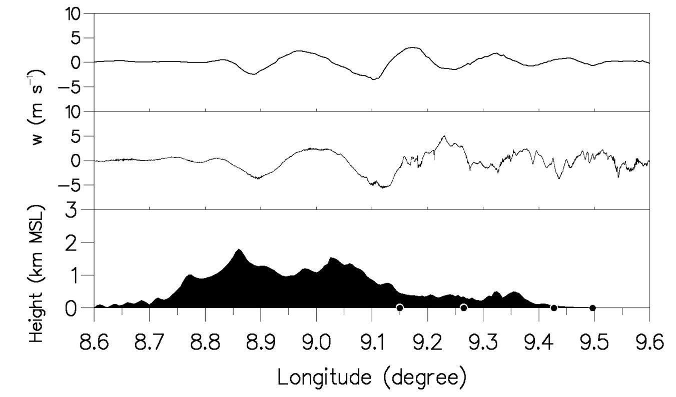

Fig. 2: Vertical velocity from simulations (top) and aircraft flights (middle) as well as orography (bottom) along flight track (see Fig. 1). Observations and simulations are at 3 km MSL and 1130 UTC. Positions of Corte, Pont génois, Casaperta and Aléria (from west to east, black dots) are indicated.

(i) COSMO simulations and (ii) model validation

(i) COSMO simulations

- high-resolution simulations (500 m grid spacing) nested in 2.8 km runs

(ii) Model validation

COSMO reproduces the main observed features:

- mountain waves (Fig. 2)

Valley (Corte, Figs. 3a,b and 4)

- 0800 UTC: abrupt decrease of humidity, increase of wind speed and change of wind direction, strong increase of ABL depth, z_{BRN} (*), onset of downward motion
- 1430 UTC: change of wind direction, increase of humidity, strong upward motion

Coast (San Giuliano, Fig. 3c,d)

- shallow ABL throughout the day

(*) z_{BRN} is calculation based on Bulk-Richardson number $BRN = \frac{gz}{\Theta} \frac{\Delta\Theta}{(u^2+v^2)}$

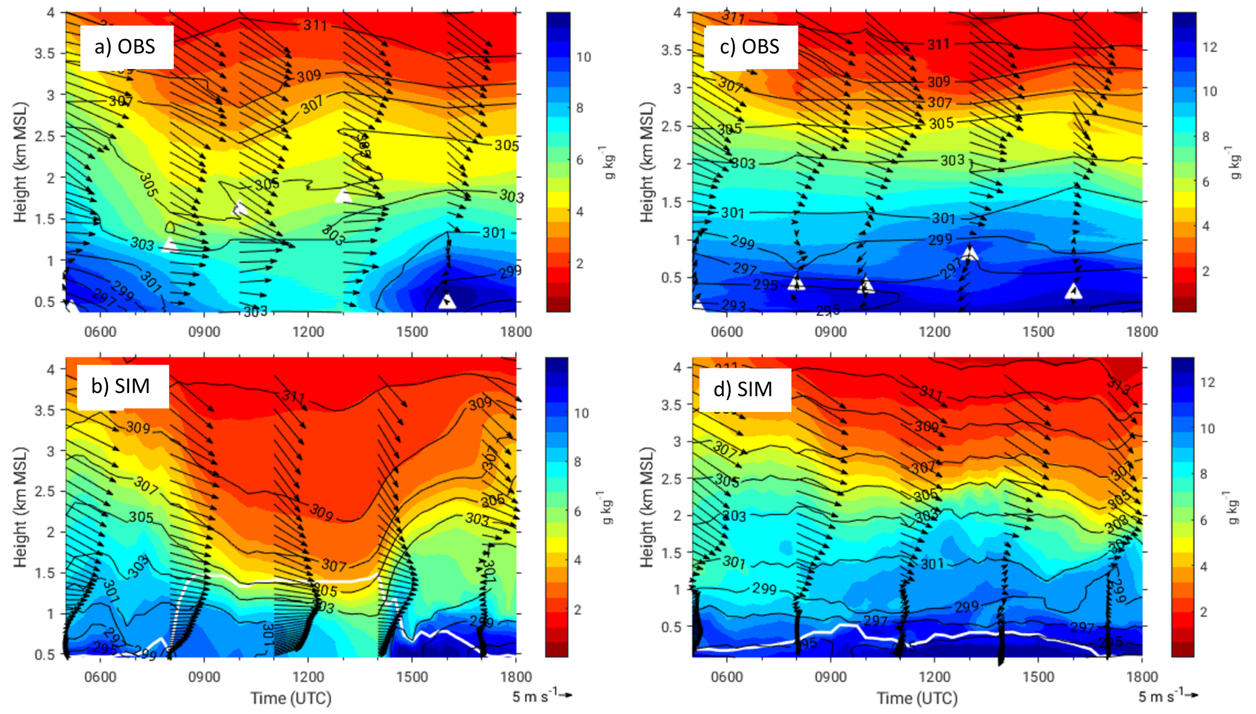

Fig. 3: Specific humidity (colour-coded), potential temperature (black isolines) and horizontal wind (arrows) measured (a) and simulated (b) at Corte and measured (c) and simulated (d) at San Giuliano. In (a) and (c), the ABL depth, z_{BRN}, is indicated by triangles and in (b) and (d) by solid white lines.

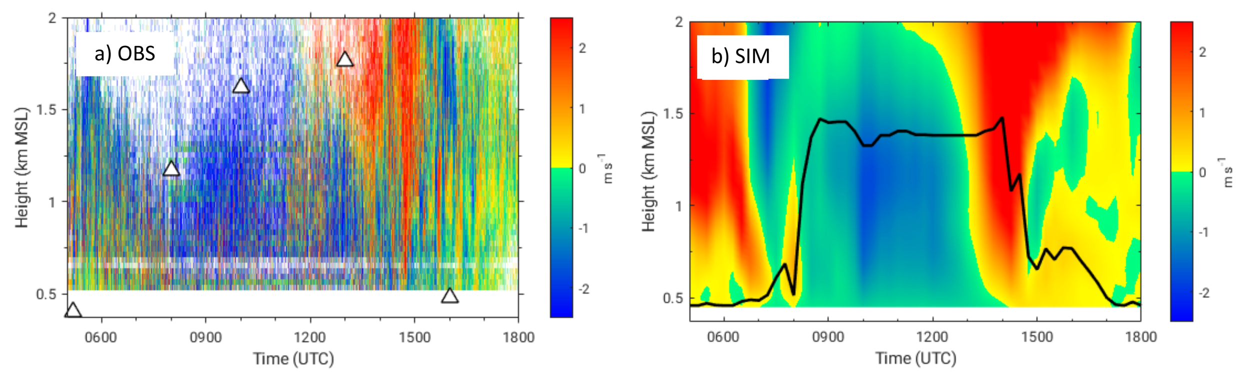

Fig. 4: Measured vertical velocity (colour coded) (a) and simulated (b) for Corte. In (a), z_{BRN} is indicated by triangles and in (b) by a solid black line.

(iii) Interpretation of ABL development at measurement sites

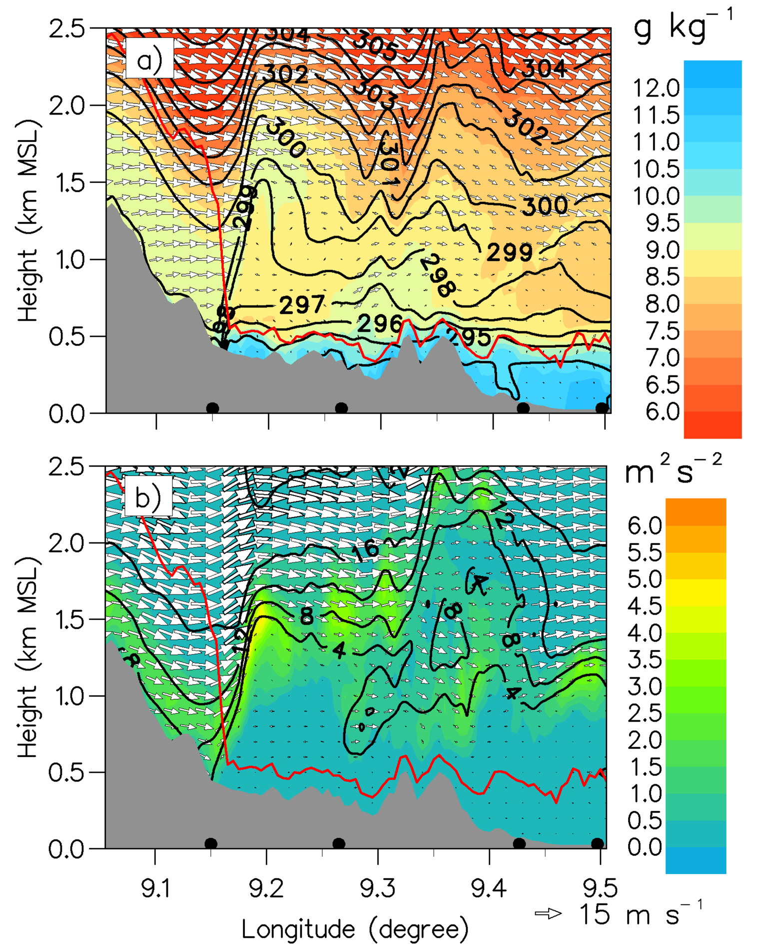

Fig. 5: 0830 UTC: (a) simulated specific humidity (colour coded), potential temperature (isolines), u,v-wind vector (arrows) and (b) TKE (colour coded), absolute value of horizontal wind speed (isolines), u,w-wind vector (arrows, the w-component is multiplied by a factor of 3) and z_{BRN} (solid red line). The cross sections are along the flight track (see Fig. 1). The positions of Corte, Pont génois, Casaperta and Aléria (west to east) are marked as black dots.

0800 UTC:

- the nocturnal surface inversion was eroded by surface-based buoyancy- and shear-driven turbulence from below and by wave-generated turbulence from above (Fig. 5).
- the mountain wave penetrated down to the surface causing the observed deep ABL (Figs. 3 and 4). The marked downward motion (Fig. 4) was caused by the downward directed branch of the wave (Fig. 5).

1430 UTC:

- the westward propagating sea breeze reached Corte (Fig. 6).
- convergence between westerly flow in the mountain wave and the easterly flow in the upvalley propagating sea breeze (Fig. 6), led to strong upward motion (Fig. 4).

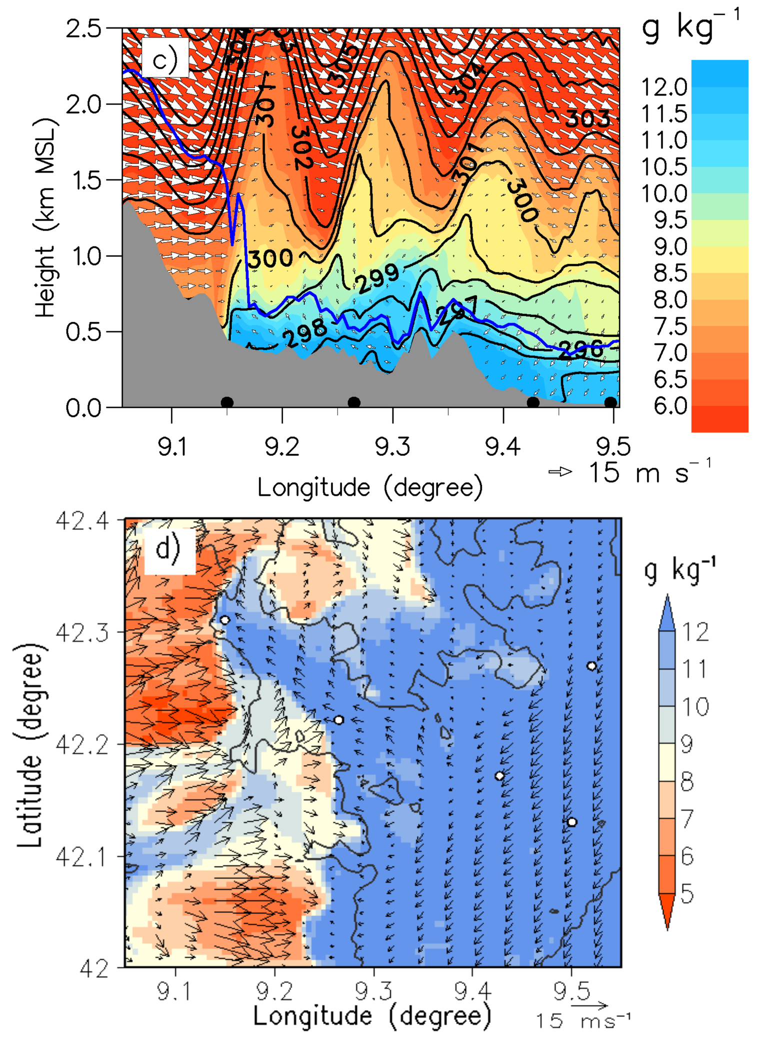

Fig. 6: 1430 UTC: (a) simulated specific humidity (colour coded), potential temperature (isolines), u,v-wind vector (allows) and z_{BRN} (solid blue line). The cross section is along the flight track (see Fig. 1). (b) Horizontal wind speed at 10 m AGL (arrows) and specific humidity at 2 m AGL (colour coded). The 600 m-contour line is highlighted (black solid line). Dots mark the five measurement stations (see Fig. 1).

(iv) Investigation of ABL characteristics along the valley

- considerable spatial differences of ABL depth at noontime in the upper part of the valley and more homogeneous distribution of ABL depth along the coast (Fig.7).

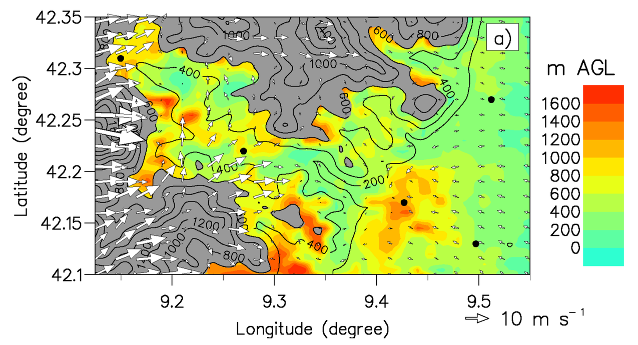

Fig. 7:Simulated spatial distribution of z_{BRN} (colour-coded) in the valley (terrain heights < 600 m MSL), terrain heights (black isolines) and horizontal wind at 10 m AGL (arrows) at 1100 UTC.

- considerable variability of ABL depth even on scales of a few kilometers (Fig. 8).

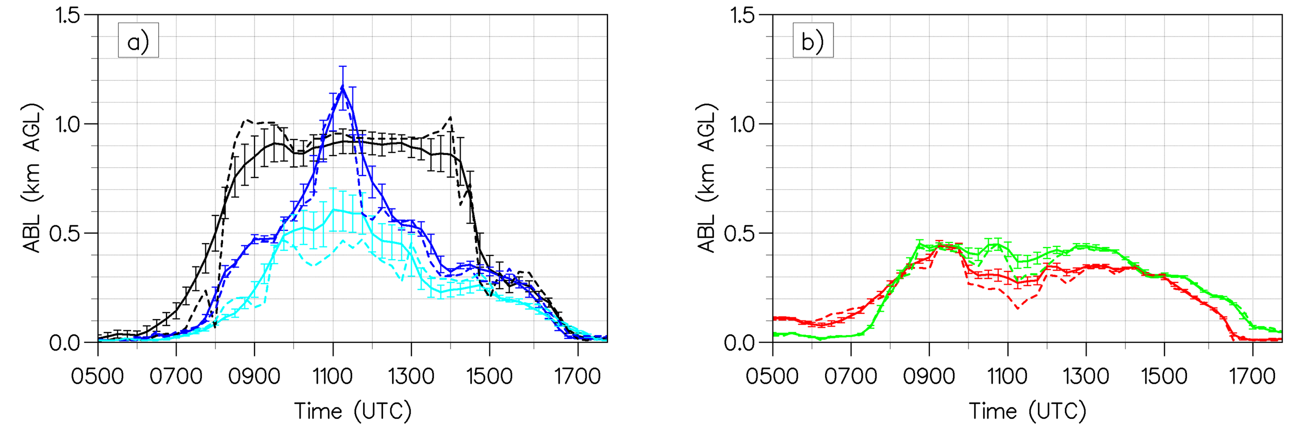

Fig. 8: Simulated mean ABL depth, $\overline{z_{BRN}}$, (solid lines), their standard deviations, $\sigma_{z_{BRN}}$, (error bars) and the individual ABL depths (dashed lines) for Corte (black), Pont génois (light blue) and Casaperta (dark blue) (a) and San Giuliano (red) and Aléria (green) (b). The mean and $\sigma_{z_{BRN}}$ values are calculated from an area consisting of 7 x 7 model grid points (approx. 12 km^2) centred around the individual sites.

- ABL depth is controlled by surface sensible heat flux, mountain wave and sea breeze (all active at noontime at Casaperta (Fig. 9).

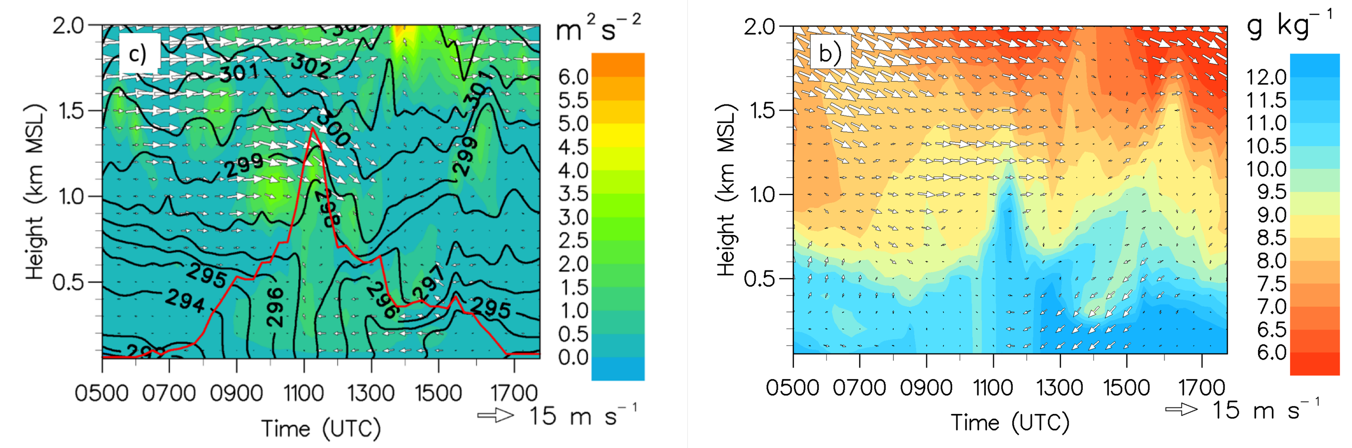

Fig. 9: (a) Simulated potential temperature (isolines), TKE (colour coded), u,w-wind vector (arrows, w component multiplied by a factor of 3) and z_{BRN} (solid red line), and (b) specific humidity (colour coded) and u,v-wind vector (arrows) at Casaperta.

- ABL depth depends on the SST. The sea breeze reaches the head of the valley earlier / later, when the SST was reduced / enhanced by 3 °C (Fig. 10) and determines the ABL depth.

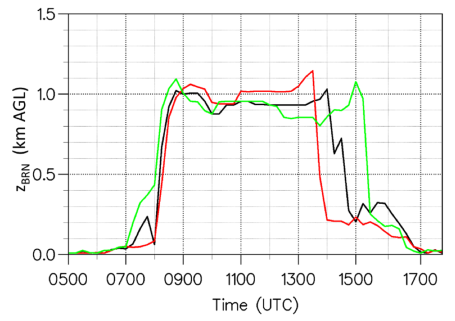

Fig. 10: Simulated ABL depth z_{BRN} at Corte for the reference run (black) and the runs with SST - 3 °C (red) and SST + 3 °C (green) compared to the reference run.

Further reading:
Adler, B., Kalthoff, N., 2016: The impact of upstream flow on the atmospheric boundary layer in a valley on a mountainous island. Boundary-Layer Meteor., 158, 429–452.
Kalthoff, N, Adler, B., Bischoff-Gauß, I., 2020: Spatio-temporal structure of the boundary layer under the impact of mountain waves. Meteorol. Z. accepted.